

BRDF Interpolation using Anisotropic Stencils

Radomír Vávra, Jiří Filip

Institute of Information Theory and Automation of the Czech Academy of Sciences, Prague, The Czech Republic

Abstract

Fast and reliable measurement of material appearance is crucial for many applications ranging from virtual prototyping to visual quality control. The most common appearance representation is BRDF capturing illumination- and viewing-dependent reflectance. One of the approaches to rapid BRDF measurement captures its subspace, using so called slices, by continuous movements of a light and camera in azimuthal directions, while their elevations remain fixed. This records set of slices in the BRDF space while remaining data are unknown. We present a novel approach to BRDF reconstruction based on a concept of anisotropic stencils interpolating values along predicted locations of anisotropic highlights. Our method marks an improvement over the original linear interpolation method, and thus we ascertain it to be a promising variant of interpolation from such sparse yet very effective measurements.

Introduction

Efficient material appearance acquisition and representation is one of the ultimate goals in computer graphics. Since the appearance acquisition process demands considerable time and resources, the introduction of more efficient measurement methods is a must. As such approaches rely on a very limited collection of reflectance samples, a reconstruction of the missing non-measured values has to be applied. This paper builds on our previously published appearance measurement based on BRDF slices [1]; however, the original reconstruction method is further extended using the concept of anisotropic stencils.

In this paper we study global material reflectance represented by the Bidirectional Reflectance Distribution Function (BRDF) as introduced by Nicodemus et al. [2]. It describes the ratio of energy reflected by material for a certain combination of incoming and outgoing directions. When we assume the separate processing of color channels, the anisotropic BRDF is a four-dimensional function $B(\theta_i, \varphi_i, \theta_v, \varphi_v)$, whereas the isotropic BRDF is merely three-dimensional, i.e., $B(\theta_i, \theta_v, |\varphi_i - \varphi_v|)$. The four dimensional anisotropic BRDF can be parameterized by two vectors specified by θ elevation and φ azimuthal angles. The vectors of illumination direction $\omega_i = (\theta_i, \varphi_i) = [x_i, y_i, z_i]$ and view direction $\omega_v = (\theta_v, \varphi_v) = [x_v, y_v, z_v]$. Anisotropic BRDF unfolded into 2D image is shown in Fig. 1-left. The image consists of toroidal subimages representing azimuthally-dependent (φ_i, φ_v) reflectance behavior for fixed view and illumination elevations (θ_i, θ_v) .

Related Work

Most BRDF related research is concentrated on isotropic BRDF due to their lower dimensionality and better availability via the MERL database [3]; therefore until recently [4], anisotropic BRDFs were used only sporadically. Although one can directly use recent anisotropic BRDF models for fitting sparse anisotropic

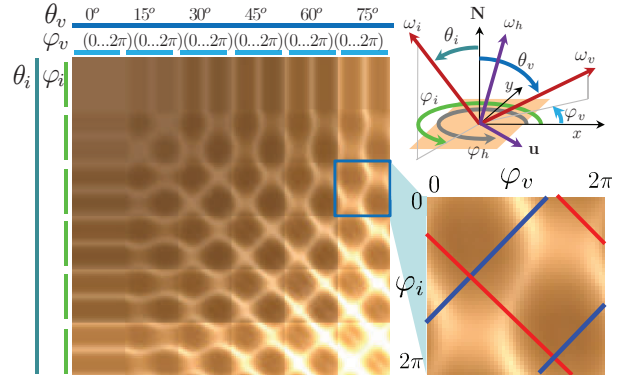


Figure 1. The 4D BRDF unfolding into 2D image (left), diagonal (blue) and axial (red) slices in a toroidal BRDF subspace (right).

measurements and reconstruction of the underlying BRDF [5], [6], the final result depends heavily either on the selection of initial parameters or on the expert knowledge of material structure and its physical properties. This is even more difficult when multiple anisotropic modes are present.

BRDF Slices

Therefore, we use the concept of BRDF slices first introduced in [1]. It suggests the reconstruction of each toroidal BRDF subspace (subimage) by means of two slices in azimuthal space as shown in Fig. 1-right. The axial slice s_A (shown as red) is measured using rotation of the mutually fixed light and sensor around the sample, while the diagonal slice s_D data (shown as blue) is obtained by mutually opposed movements of the light and sensor relative to the sample. Both the camera and light travel full circle around the sample and return to the initial position. This can be formalized using the following equations

$$\begin{aligned} s_{A, \theta_i, \theta_v, \alpha}(\varphi_v) &= B(\theta_i, \varphi_i = \varphi_v - \alpha, \theta_v, \varphi_v), \\ s_{D, \theta_i, \theta_v, \beta}(\varphi_v) &= B(\theta_i, \varphi_i = 2\pi - \varphi_v + \beta, \theta_v, \varphi_v). \end{aligned} \quad (1)$$

where α and β are initial azimuthal differences between directions to camera and light. This method was further generalized to more slices in [7].

Slices for Fast BRDF Measurement

The main advantage of BRDF slices is that they can be captured by a continuous rotation of arms holding camera and light, which significantly reduces acquisition time of the appearance data. This was practically shown in [8], where an approximate BRDF/BTF acquisition setup was introduced based on a simple, affordable mechanical gantry containing a consumer camera and two LED lights. Depiction of the initial prototype setup and its

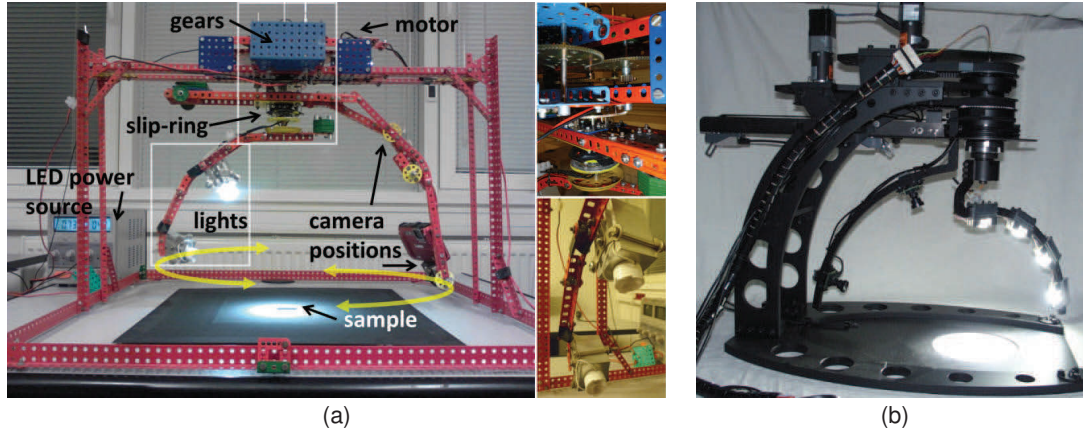


Figure 2. Measurement devices: (a) an initial proof-of-concept device build from a toy-construction set [8], and (b) a fully automatic prototype of a commercial solution.

subsequent fully automatic successor are shown in Fig. 2. The device is portable and can be folded down to luggage size.

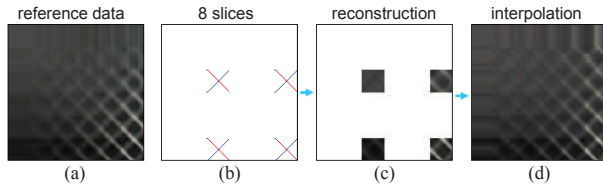


Figure 3. A principle of entire BRDF reconstruction from four recorded subspaces [1]: (a) the reference, (b) sparse-sampling of eight slices, (c) reconstructions of elevations where the slices were measured, (d) missing data interpolation.

It captures a very limited subset of material surface images by shooting several video sequences in less than four minutes. The BRDF space is sampled only sparsely and the majority of its values are unmeasured. The missing data reconstruction method presented in [7] allows for a fast, inexpensive, acquisition of approximate BRDFs/BTFs (Fig. 3) from two slices per subspace; however, as it uses only a constrained linear interpolation method [1], [7], it provides only an approximate reconstruction of appearance representation as shown in Fig. 4. This effect is most apparent at subspaces with significant difference between illumination and viewing angles, i.e., $|\theta_i - \theta_v| > 45^\circ$. The anisotropic highlights at such elevations are not perpendicular to the slices and the original orthogonal linear projection method [7] cannot provide proper results.

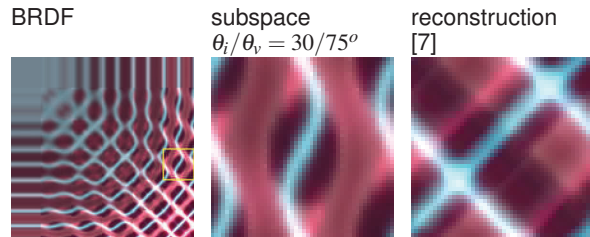


Figure 4. A BRDF subspace reconstruction error for $|\theta_i - \theta_v| = 45^\circ$.

Our Contribution

Therefore, in this paper we strive to improve BRDF reconstruction from two slices per subspace. We build on a recent paper [9] predicting locations of anisotropic highlights in the BRDF space. The locations of anisotropic highlights can be predicted [10] on directional surface elements laying in planes orthogonal to the bisector (often denoted as half-way direction $\omega_h = \frac{\omega_i + \omega_v}{\|\omega_i + \omega_v\|} = (\theta_h, \phi_h)$) of directions of incidence and reflectance as proposed in [11]. Therefore, anisotropic highlights can be predicted at directions of the bisector orthogonal to the detected anisotropy axis of the material $\mathbf{u} = [\sin \phi_h, \cos \phi_h, 0]$, i.e., $\omega_h \cdot \mathbf{u} = 0$. An example of predicted locations of anisotropic highlights are shown in Fig. 5, BRDFs and their rendering for four different anisotropy alignment angles ϕ_h are shown side-by-side with prediction of locations of one of the anisotropic highlights in directional space.

The technique of anisotropic highlights (so called anisotropic stencils) prediction was successfully applied to the efficient modeling of highly anisotropic BRDFs featuring multi-axial anisotropy [12]. The main advantage of such a model is its extremely fast and reliable fitting of anisotropic highlights without the need of using iterative optimization techniques.

In the following section we outline a BRDF data interpolation method based on anisotropic stencils, i.e., benefiting from prior analytical knowledge of an anisotropic highlights location.

Proposed Interpolation Method

Our interpolation method is based on the observation that BRDF values are almost constant along azimuthal angle ϕ_h of half-way direction ω_h . Therefore, each reconstructed point P in the BRDF subspace can be interpolated from the point on diagonal slice (A) and the point on axial slice (B) with the same ϕ_h as shown in Fig. 6-right.

We will derive equations to find coordinates in azimuthal space (ϕ_i, ϕ_v) for both points. First, let us remind basic equations for conversions between the spherical and Cartesian coordinates:

$$\begin{aligned} x &= \sin(\theta) \cdot \cos(\varphi), & \theta &= \arccos(z) \\ y &= \sin(\theta) \cdot \sin(\varphi), & \varphi &= \arctan\left(\frac{y}{x}\right) \\ z &= \cos(\theta). \end{aligned} \quad (2)$$

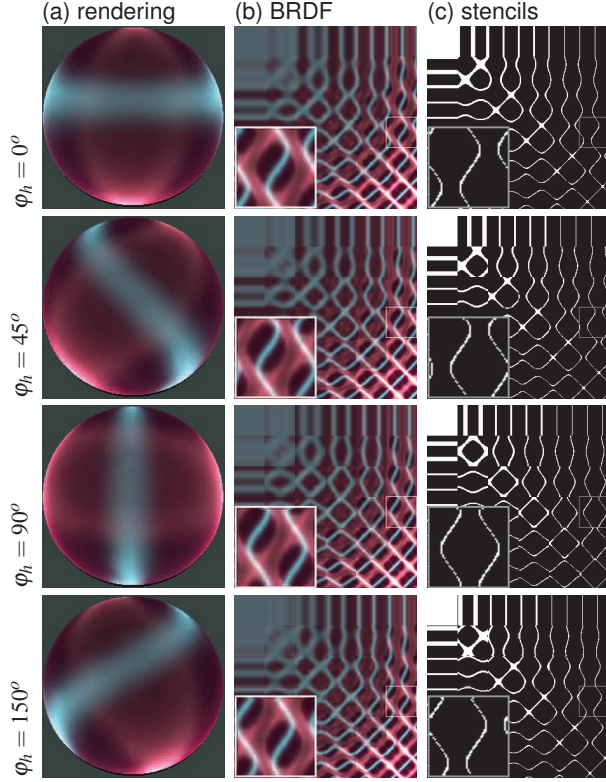


Figure 5. Anisotropic highlights alignment within BRDF coordinate system for different directions of anisotropy $\varphi_h = 0/45/90/150^\circ$. The BRDF rendered on a sphere and prediction of anisotropic highlights locations (stencils) for anisotropy alignment of blue highlights.

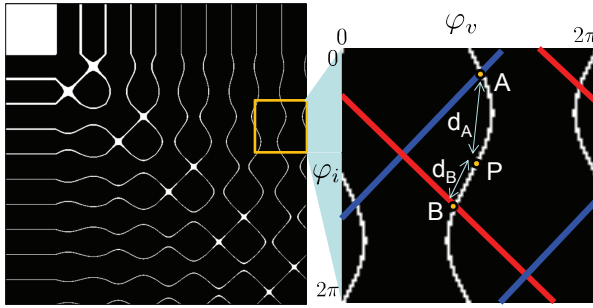


Figure 6. BRDF slices interpolation along anisotropic stencil.

Elevation angles are fixed across the subspace where interpolation is performed $\theta_i^A = \theta_i^B = \theta_i^P$, $\theta_v^A = \theta_v^B = \theta_v^P$.

The alignment angle φ_h of the stencil intersecting the reconstructed point can be obtained as:

$$\varphi_h^P = \arctan\left(\frac{y_i^P + y_v^P}{x_i^P + x_v^P}\right), \quad (3)$$

To find the point B (φ_i^B, φ_v^B) with $\varphi_h^B = \varphi_h^P$ on the axial slice we create a system of equations:

$$\begin{aligned} \varphi_i^B &= \varphi_v^B - \alpha, \\ \varphi_h^B &= \arctan\left(\frac{y_i^B + y_v^B}{x_i^B + x_v^B}\right). \end{aligned} \quad (4)$$

Similar equations can be derived for the point A (φ_i^A, φ_v^A) on the diagonal slice:

$$\begin{aligned} \varphi_i^A &= 2\pi - \varphi_v^A + \beta, \\ \varphi_h^A &= \arctan\left(\frac{y_i^A + y_v^A}{x_i^A + x_v^A}\right). \end{aligned} \quad (5)$$

The solution of the equations is:

$$\begin{aligned} \varphi_v^A &= \arctan\left(\frac{C_1 + C_3(\beta) + C_4(\beta)}{C_2 + C_5(\beta) - C_6(\beta)}\right), \\ \varphi_v^B &= \arctan\left(\frac{C_1 + C_3(\alpha) - C_4(\alpha)}{C_2 - C_5(\alpha) - C_6(\alpha)}\right), \end{aligned} \quad (6)$$

where

$$\begin{aligned} C_1 &= \sin(\theta_v^P) \cdot \sin(\varphi_h^P), \\ C_2 &= \sin(\theta_v^P) \cdot \cos(\varphi_h^P), \\ C_3(v) &= \sin(\theta_i^P) \cdot \cos(v) \cdot \sin(\varphi_h^P), \\ C_4(v) &= \sin(\theta_i^P) \cdot \sin(v) \cdot \cos(\varphi_h^P), \\ C_5(v) &= \sin(\theta_i^P) \cdot \cos(v) \cdot \cos(\varphi_h^P), \\ C_6(v) &= \sin(\theta_i^P) \cdot \sin(v) \cdot \sin(\varphi_h^P). \end{aligned} \quad (7)$$

As the viewing and illumination azimuthal angles are coupled by means of initial difference between azimuthal angles prior to the measurement (α for the axial slice, β for the diagonal slice), we can also obtain a corresponding illuminations azimuths φ_i for diagonal and axial slices using equations (4) and (5) respectively.

Finally, we can reconstruct the unknown reflectance value P using Euclidean-weighted linear combination of reflectance values at points A and B

$$P(\varphi_i, \varphi_v) = s_A(\varphi_v^B) \frac{d_A}{d_A + d_B} + s_D(\varphi_v^A) \frac{d_B}{d_A + d_B}, \quad (8)$$

where d_A, d_B are Euclidean distances of point P to points A, B in azimuthal space (see Fig. 6-right).

Test Dataset

As the number of publicly available anisotropic BRDFs is limited, we resorted to the UTIA BRDF Database¹ [4] as the only source of a reasonable number of different types of anisotropic BRDF measurements. This database contains 150 BRDFs of fabric, wood, leather, plastic and paint materials; out of which, over 40 exhibit some strong visual aspect of anisotropy [13]. The BRDFs are stored in HDR format, and their angular resolution is 15° in elevations and 7.5° in azimuthal angles.

As our reconstruction method is currently beneficial only to anisotropic BRDFs, we analyzed the variance along axial slices in all BRDF subspaces of the entire 150 BRDFs in order to only detect those having significant anisotropic behavior. Out of these 150 BRDFs we eventually selected 37 anisotropic BRDFs to test our reconstruction method. See an example of anisotropic BRDF of material *fabric094* in Fig. 7-a.

For the purpose of reconstruction we kept only samples lying in the slices (see Fig. 1-right). As one slice covers 360° by 48 samples using azimuthal sampling step 7.5° , we obtain $48 \times 48 = 96$ samples for each subspace for fixed combination of θ_i/θ_v .

¹<http://btf.utia.cas.cz>

The elevation step 15° samples 90° using 6 values. This gives us $6 \times 6 = 36$ subspaces and total number of $36 \times 96 = 3456$ samples. However this number reduces, due to illumination and view reciprocity to 1842 samples. Further, the subspaces where the elevation angles are zero can be sufficiently sampled by means of one slice only, while for representation of subspace $\theta_i = \theta_v = 0^\circ$ only one sample is needed, which saves 287 samples. Thus finally only $1842 - 287 = 1555$ samples is used for the reconstruction of the original BRDF (see Fig. 7-b).

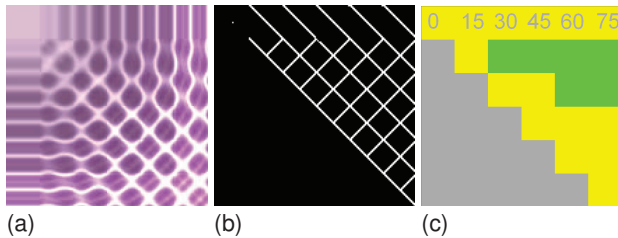


Figure 7. Example BRDF (a), a mask showing distribution of 1555 samples in two slices per subspace (b), and distribution of subspaces reconstructed by the original approach (yellow) and by the proposed approach (green) (c).

Our reconstruction method, due to discontinuities in anisotropic stencils, does not work properly when view and illumination elevation angles are approximately equal. Therefore, in this case we use the original interpolation approach [7]. For the experiment, we settled at using our method for elevations as denoted by green and using the original method at elevations as denoted by yellow shown in Fig. 7-c. On the other hand, the original approach works quite well in this case as both specular and anisotropic highlights are perpendicular to the slices and thus can be easily reproduced by their orthogonal projection.

Results and Discussion

A performance of the proposed reconstruction method as compared to the original method [7] for eight subspaces of anisotropic BRDFs (elevations $\theta_i = 30^\circ$, $\theta_v = 75^\circ$) are shown in Fig. 8. One can observe an inaccurate reconstruction of subspaces by means of the original method (b), while the proposed approach (c), when compared to the reference (a), works reasonably well.

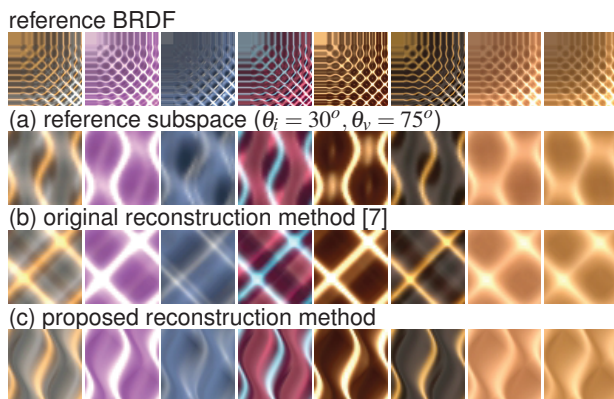


Figure 8. A comparison of (a) BRDF subspace $\theta_i = 30^\circ$, $\theta_v = 75^\circ$ reconstruction using the (b) original and (c) the proposed methods.

Results of a reconstructed BRDF rendering on a sphere il-

luminated from front and left respectively together with corresponding PSNR values are shown in Figs. 9 and 10. Again our approach (third column) demonstrates an improvement over the original method (second column).

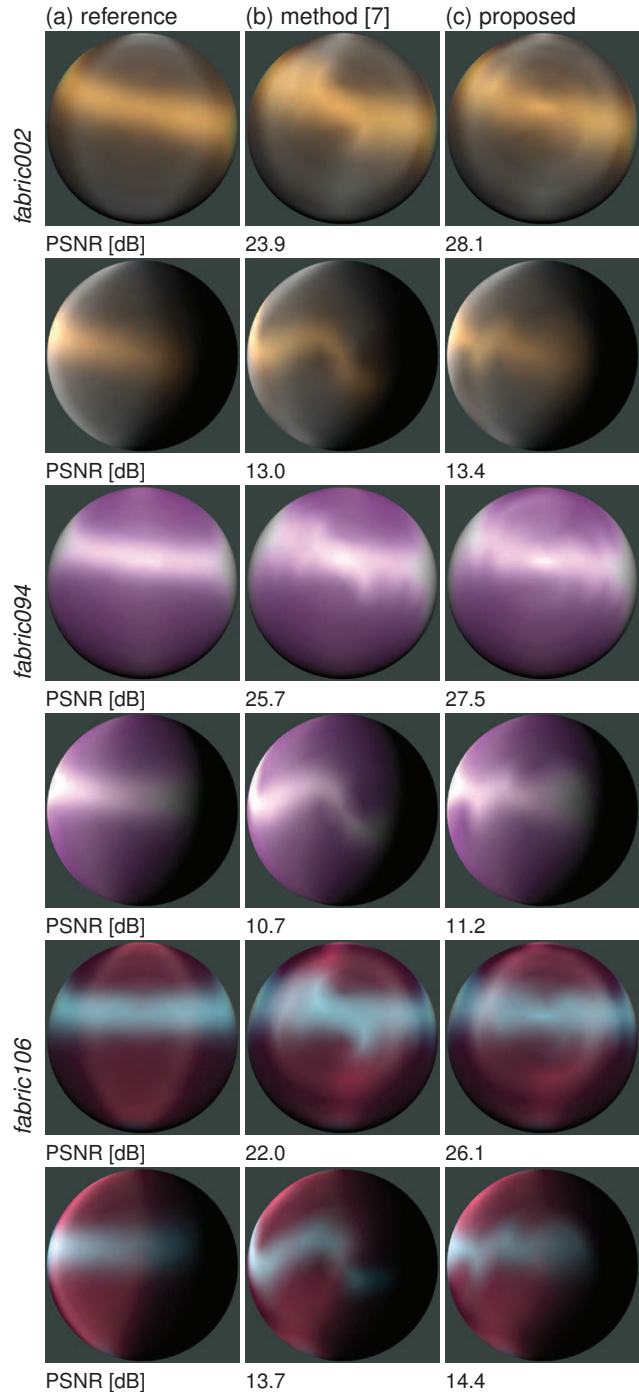


Figure 9. Comparing BRDFs and their respective rendering on sphere of two methods of slices interpolation: (a) reference, (b) its reconstruction from two slices per subspace using the original slices interpolation technique [7], (c) the proposed anisotropic stencils-based technique.

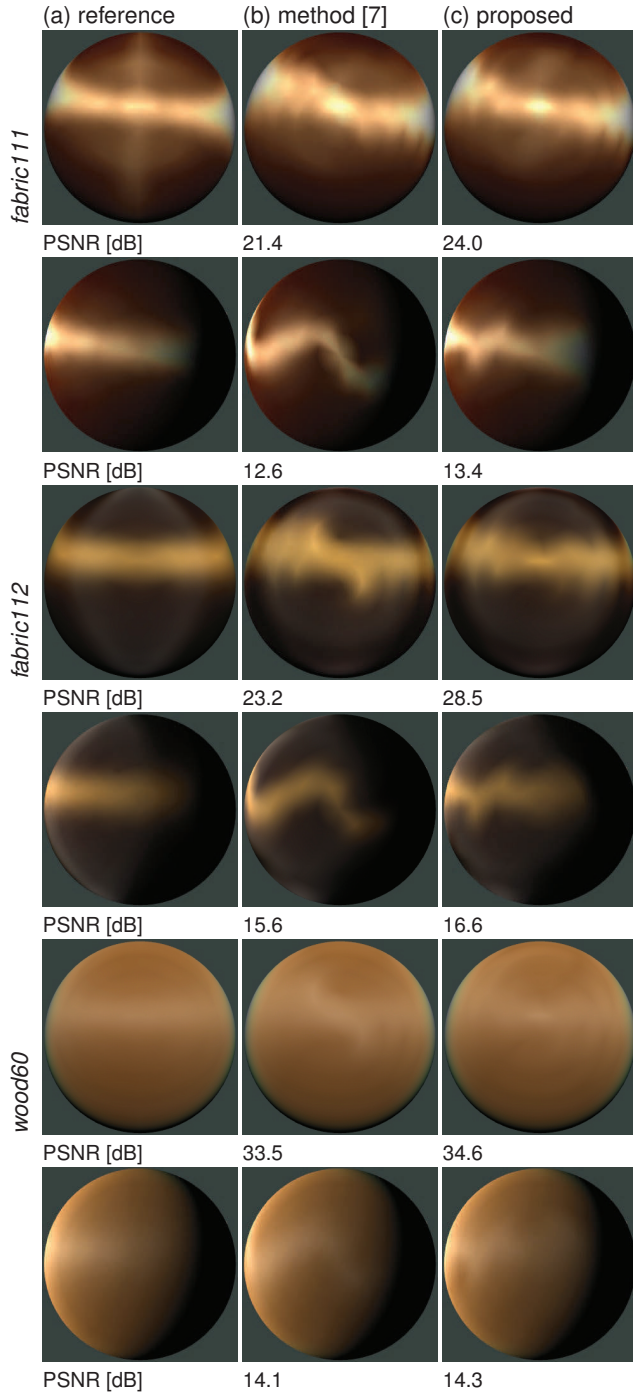


Figure 10. Comparing BRDFs and their respective rendering on sphere of two methods of slices interpolation: (a) reference, (b) its reconstruction from two slices per subspace using the original slices interpolation technique [7], (c) the proposed anisotropic stencils-based technique.

Three of the tested fabric materials illuminated by environment illumination *grace* are shown in Fig. 12. These results also demonstrate a considerable quality gain achieved by using of our method when compared to the original one.

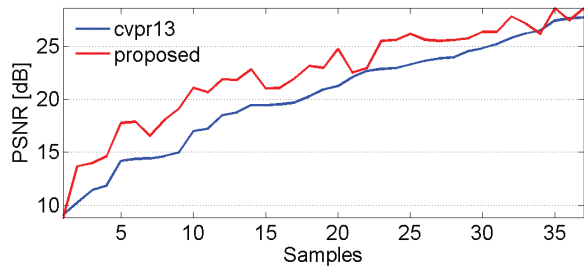


Figure 11. Performance of our method across 37 anisotropic BRDFs.

Finally, Fig. 11 shows a graph comparing performance of both methods across all 37 tested anisotropic BRDFs. One can observe steady reconstruction improvement of the proposed method over the original solution.

As no demanding computation is involved the computational costs of the proposed reconstruction method are comparable with the original one and take approx 1s in our MATLAB implementation.

Limitations

As the results suggest, our method has currently several limitations. First, it does not work properly if the material is isotropic or nearly isotropic. This can be avoided by data analysis across axial slices when one can directly detect material anisotropy [13] and use this information to toggle between original and proposed method. Second, for a subspace having low difference $|\theta_i - \theta_v|$ the original method performs better. We assume that performance of our method in such conditions can be further improved by the analytical computation of interpolation weight coefficients along the anisotropic highlights, e.g., along length of highlight curve.

Conclusions

We proposed a novel method of BRDF reconstruction from continuously measured slices. The main benefit of such measurement lies in very efficient and affordable acquisition. The method's thorough comparison with the baseline approach has shown that it achieves a consistently better performance. We consider our reconstruction results to be especially encouraging and as in initial achievement in making way for more efficient material appearance capturing methods.

In a future work we plan to extend our approach to the general interpolation of anisotropic BRDFs from any sparsely distributed samples.

Acknowledgments

This research has been supported by the Czech Science Foundation grant 14-02652S.

References

- [1] J. Filip and R. Vávra, "Fast method of sparse acquisition and reconstruction of view and illumination dependent datasets," *Computer and Graphics*, vol. 37, no. 5, pp. 376–388, 2013.
- [2] F. Nicodemus, J. Richmond, J. Hsia, I. Ginsburg, and T. Limperis, "Geometrical considerations and nomenclature for reflectance," *NBS Monograph 160, National Bureau of Standards, U.S. Dept. of Com.*, pp. 1–52, 1977.
- [3] W. Matusik, H. Pfister, M. Brand, and L. McMillan, "A

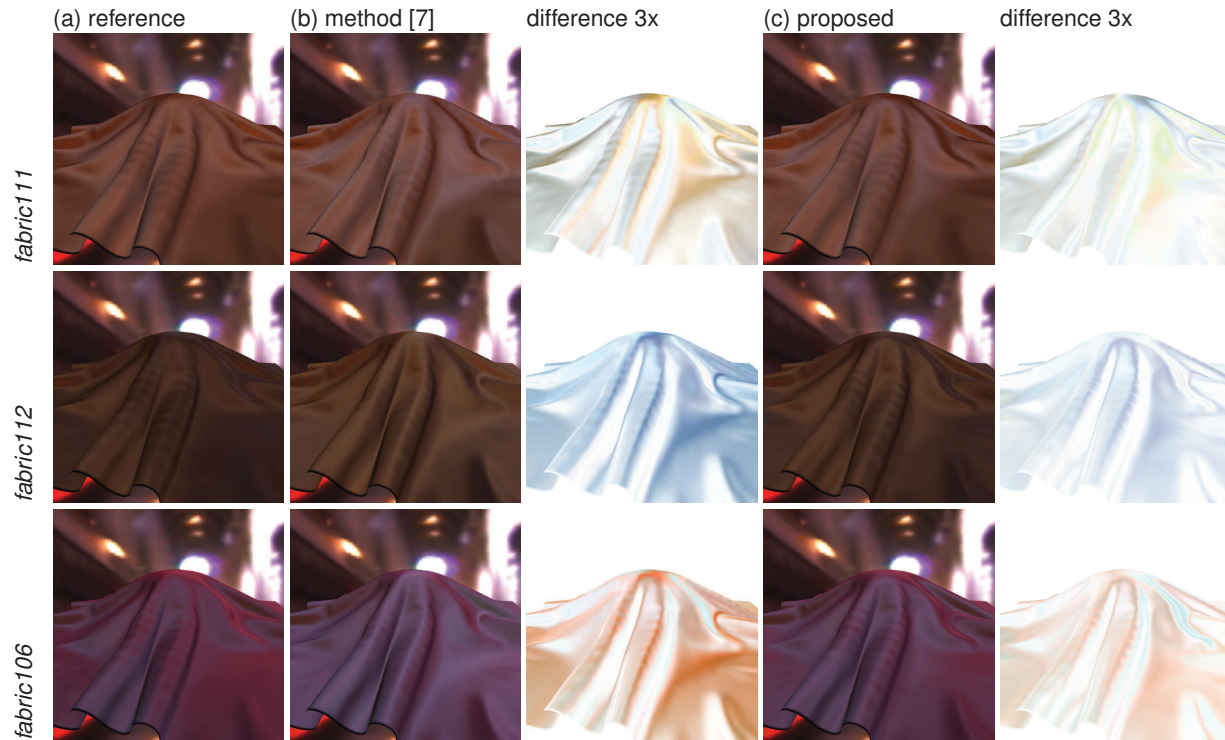


Figure 12. Rendering of three fabric materials in illumination environment: (a) reference BRDF, (b) original reconstruction method [7], (c) the proposed method.

- data-driven reflectance model,” *ACM Trans. Graph.*, vol. 22, no. 3, pp. 759–769, 2003.
- [4] J. Filip and R. Vávra, “Template-based sampling of anisotropic BRDFs,” *Computer Graphics Forum*, vol. 33, no. 7, pp. 91–99, October 2014.
 - [5] M. Kurt, L. Szirmay-Kalos, and J. Křivánek, “An anisotropic BRDF model for fitting and monte carlo rendering,” *SIGGRAPH Comput. Graph.*, vol. 44, pp. 3:1–3:15, February 2010.
 - [6] I. Sadeghi, O. Bisker, J. De Deken, and H. W. Jensen, “A practical microcylinder appearance model for cloth rendering,” *ACM Trans. Graph.*, vol. 32, no. 2, pp. 14:1–14:12, Apr. 2013.
 - [7] J. Filip, R. Vávra, M. Haindl, P. Žid, M. Krupička, and V. Havran, “BRDF slices: Accurate adaptive anisotropic appearance acquisition,” in *CVPR 2013*, 2013, pp. 4321–4326.
 - [8] J. Filip, R. Vávra, and M. Krupička, “Rapid material appearance acquisition using consumer hardware,” *Sensors*, vol. 14, no. 10, pp. 19 785–19 805, 2014.
 - [9] J. Filip and R. Vávra, “Anisotropic materials appearance analysis using ellipsoidal mirror,” in *IS&T/SPIE Conference on Measuring, Modeling, and Reproducing Material Appearance*, paper 9398-25, February 2015.
 - [10] B. Raymond, G. Guennebaud, P. Barla, R. Pacanowski, and X. Granier, “Optimizing BRDF orientations for the manipulation of anisotropic highlights,” in *Computer Graphics Forum*, vol. 33, no. 2, 2014, pp. 313–321.
 - [11] R. Lu, J. J. Koenderink, and A. M. Kappers, “Specularities on surfaces with tangential hairs or grooves,” *Computer Vision and Image Understanding*, vol. 78, no. 3, pp. 320–335, 2000.
 - [12] J. Filip, M. Havlíček, and R. Vávra, “Adaptive highlights stencils for modeling of multi-axial BRDF anisotropy,” *To appear in The Visual Computer*, 2015.
 - [13] J. Filip, “Analyzing and predicting anisotropic effects of BRDFs,” in *Proceedings of the ACM SIGGRAPH Symposium on Applied Perception*, ser. SAP ’15, 2015, pp. 25–32.

Author Biography

Radomír Vávra received the MSc from the Czech Technical University in Prague. He currently works as a PhD candidate at Institute of Information Theory and Automation (UTIA) of the Czech Academy of Sciences. His research interest includes accurate material appearance measurement techniques and material visualization methods in computer graphics.

Jiří Filip received the MSc and PhD, both in cybernetics from the Czech Technical University in Prague. Since 2002 he is a researcher at the Institute of Information Theory and Automation (UTIA) of the Czech Academy of Sciences. Between 2007-2009 he was Marie-Curie research fellow at Heriot-Watt University, Edinburgh. He combines methods of image processing, computer graphics, and visual psychophysics. His current research is focused on precise measurement, and modeling of material appearance.